

Recursion formula for reflectance and the enhanced effect on the light group velocity control of the stratified and phase-shifted volume index gratings

Guoquan Zhang, Weiyue Che, Bin Han, and Yiling Qi

Photonics Center, College of Physics Science, Nankai University, Tianjin 300071, China
and The Key Laboratory of Advanced Technique and Fabrication for Weak-Light Nonlinear
Photonics Materials, Ministry of Education, Nankai University, Tianjin 300457, China
and Tianjin Key Laboratory of Photonics Materials and Technology for Information Science,
Nankai University, Tianjin 300457, China

zhanggq@nankai.edu.cn

Abstract: We derived a recursion formula for the reflectance of the stratified and phase-shifted volume index gratings. The characteristics of the reflectance spectra of the stratified and phase-shifted volume index gratings were studied based on the recursion formula. It is shown that narrow bandwidth transparency peaks appear within the stop-band of the reflectance spectrum of the volume index gratings due to the intervention of the homogeneous buffer layers that induce the phase-shifts between neighboring volume index gratings. The spectral positions of the transparency peaks can be shifted within the stop-band by controlling the phase-shift, i.e., the buffer layer thickness. The described properties may find applications in addressable band-pass filter, switching, wavelength division multiplexing, and de-multiplexing. The dispersion near the transparency peaks of the stratified and phase-shifted volume index grating is found to be sharply enhanced as compared to the uniform volume index gratings. Significantly enhanced control on the group velocity of light by several orders of magnitude while keeping high transmittance is demonstrated in the stratified and phase-shifted volume index grating.

© 2007 Optical Society of America

OCIS codes: (230.4170) Multilayers; (260.2030) Dispersion; (050.2770) Gratings; (060.1810) Couplers, switches, and multiplexers.

References and links

1. P. Yeh, *Optical Waves in Layered Media* (Wiley, New York, 1988).
2. J. D. Joannopoulos, R. D. Meade, and J. N. Winn, *Photonic Crystals: Molding the Flow of Light* (Princeton University Press, Princeton, 1995).
3. R. C. Alferness, C. H. Joyner, M. D. Divino, M. J. R. Martyak, and L. L. Buhl, "Narrowband grating resonator filters in InGaAsP/InP waveguides," *Appl. Phys. Lett.* **49**, 125–127 (1986).
4. G. P. Agrawal and S. Radic, "Phase-Shifted Fiber Bragg Gratings and their Application for Wavelength Demultiplexing," *IEEE Photon. Technol. Lett.* **6**, 995–997 (1994).
5. R. Zengerle and O. Leminger, "Phase-shifted Bragg-Grating Filters with Improved Transmission Characteristics," *J. Lightwave Technol.* **13**, 2354–2358 (1995).
6. L. Wei and J. W. Y. Lit, "Phase-Shifted Bragg Grating Filters with Symmetrical Structures," *J. Lightwave Technol.* **15**, 1405–1410 (1997).

7. F. Bakhti and P. Sansonetti, "Design and Realization of Multiple Quarter-Wave Phase-Shifts UV-Written Bandpass Filter in Optical Fibers," *J. Lightwave Technol.* **15**, 1433–1437 (1997).
8. Ch. Martinez and P. Ferdinand, "Analysis of phase-shifted fiber Bragg gratings written with phase plate," *Appl. Opt.* **38**, 3223–3228 (1999).
9. S. Longhi, M. Marano, P. Laporta, O. Svelto, and M. Belmonte, "Propagation, manipulation, and control of picosecond optical pulses at 1.5 μm in fiber Bragg gratings," *J. Opt. Soc. Am B* **19**, 2742–2757 (2002).
10. Y. Painchaud, A. Chandonnet, and J. Lauzon, "Chirped fibre gratings produced by tilting the fibre," *Electron. Lett.* **31**, 171–172 (1995).
11. B. Malo, S. Thériault, D. C. Johnson, F. Bilodeau, J. Albert, and K. O. Hill, "Apodised in-fibre Bragg grating reflectors photoimprinted using a phase mask," *Electron. Lett.* **31**, 223–225 (1995).
12. Ch. Martinez, S. Magne, and P. Ferdinand, "Apodized fiber Bragg gratings manufactured with the phase plate process," *Appl. Opt.* **41**, 1733–1740 (2002).
13. R. V. Johnson, A. R. Tanguay, "Stratified volume holographic optical elements," *Opt. Lett.* **13**, 189–191 (1988).
14. G. P. Nordin, R. V. Johnson, A. R. Tanguay, "Diffraction properties of stratified volume holographic optical elements," *J. Opt. Soc. Am. A* **9**, 2206–2217 (1992).
15. R. De Vré and L. Hesselink, "Analysis of photorefractive stratified volume holographic optical elements," *J. Opt. Soc. Am. B* **11**, 1800–1808 (1994).
16. J. J. Stankus, S. M. Silence, W. E. Moerner, and G. C. Bjorklund, "Electric-field-switchable stratified volume holograms in photorefractive polymers," *Opt. Lett.* **19**, 1480–1482 (1994).
17. V. M. Petrov, C. Caraboue, J. Petter, T. Tschudi, V. V. Bryksin, and M. P. Petrov, "A dynamic narrow-band tunable optical filter," *Appl. Phys. B* **76**, 41–44 (2003).
18. Y. Lai, W. Zhang, L. Zhang, J. A. R. Williams, and I. Bennion, "Optically tunable fiber grating transmission filters," *Opt. Lett.* **28**, 2446–2448 (2003).
19. A. D'Orazio, M. De Sario, V. Petruzzelli, and F. Prudenzano, "Photonic band gap filter for wavelength division multiplexer," *Opt. Express* **11**, 230–239 (2003).
20. M. Yamada and K. Sakuda, "Analysis of almost-periodic distributed feedback slab waveguides via a fundamental matrix approach," *Appl. Opt.* **26**, 3474–3478 (1987).
21. M. McCall, "On the application of coupled mode theory for modeling fiber Bragg gratings," *J. Lightwave Technol.* **18**, 236–242 (2000).
22. M. A. Rodriguez, M. S. Malcuit, and J. J. Butler, "Transmission properties of refractive index-shifted Bragg gratings," *Opt. Commun.* **177**, 251–257 (2000).
23. S. Khorasani and K. Mehrany, "Differential transfer-matrix method for solution of one-dimensional linear non-homogeneous optical structures," *J. Opt. Soc. Am. B* **20**, 91–96 (2003).
24. S. Khorasani and A. Adibi, "New analytical approach for computation of band structure in one-dimensional periodic media," *Opt. Commun.* **216**, 439–451 (2003).
25. J. J. Monzón, T. Yonte, and L. L. Sánchez-Soto, "Characterizing the reflectance of periodic layered media," *Opt. Commun.* **218**, 43–47 (2003).
26. I. S. Nefedov and S. A. Tretyakov, "Photonic band gap structure containing metamaterial with negative permittivity and permeability," *Phys. Rev. E* **66**, 036611-1–4 (2002).
27. J. R. Birge and F. X. Kärtner, "Efficient analytic computation of dispersion from multilayer structures," *Appl. Opt.* **45**, 1478–1483 (2006).
28. D. Yevick and L. Thylén, "Analysis of gratings by the beam-propagation method," *J. Opt. Soc. Am.* **72**, 1084–1089 (1982).
29. L. Thylen and D. Yevick, "Beam propagation method in anisotropic media," *Appl. Opt.* **21**, 2751–2754 (1982).
30. L. Thylen and Ch. M. Lee, "Beam-propagation method based on matrix diagonalization," *J. Opt. Soc. Am. A* **9**, 142–146 (1992).
31. Y. Tsuji, M. Koshihara, and N. Takimoto, "Finite element beam propagation method for anisotropic optical waveguides," *J. Lightwave Technol.* **17**, 723–728 (1999).
32. P. K. Kelly and M. Piket-May, "Propagation characteristics for a one-dimensional grounded finite height finite length electromagnetic crystal," *J. Lightwave Technol.* **17**, 2008–2012 (1999).
33. L. A. Coldren and S. W. Corzine, *Diode Lasers and Photonic Integrated Circuits* (Wiley, New York, 1995).
34. M. Scalora, R. J. Flynn, S. B. Reinhardt, R. L. Fork, M. J. Bloemer, M. D. Tocci, C. M. Bowden, H. S. Ledbetter, J. M. Bendickson, and R. P. Leavitt, "Ultrashort pulse propagation at the photonic band edge: large tunable group delay with minimal distortion and loss," *Phys. Rev. E* **54**, R1078–R1081 (1996).
35. S. H. Lin, K. Y. Hsu, and P. Yeh, "Experimental observation of the slowdown of optical beams by a volume-index grating in a photorefractive LiNbO_3 crystal," *Opt. Lett.* **25**, 1582–1584 (2000).
36. S. Zhu, N. Liu, H. Zheng, and H. Chen, "Time delay of light propagation through defect modes of one-dimensional photonic band-gap structures," *Opt. Commun.* **174**, 139–144 (2000).
37. J. Liu, B. Shi, D. Zhao, and X. Wang, "Optical delay in defective photonic bandgap structures," *J. Opt. A: Pure Appl. Opt.* **4**, 636–639 (2002).
38. S. Bette, C. Caucheteur, M. Wuilpart, P. Mégret, R. Garcia-Olcina, S. Sales, and J. Capmany, "Spectral characterization of differential group delay in uniform fiber Bragg gratings," *Opt. Express* **13**, 9954–9960 (2005).

1. Introduction

The spectral properties of the periodically layered structures such as volume index gratings and one-dimension photonic crystals have been intensively studied because of their many potential applications in optical communication and information processing [1, 2]. To get a desired spectral response, modification on structure parameters such as refractive index and structure periods or structure defects is introduced to the periodically layered structure; therefore, structures such as the phase-shifted gratings [3-8], the chirped [9, 10], and the apodized gratings [11, 12] in optical fiber and the stratified volume holographic optical elements [13-16] have been proposed. Many device applications such as the narrow-bandwidth band-stop or band-pass filters [3, 5, 6, 17, 18] as well as wavelength division multiplexer and de-multiplexer [4, 19] have also been suggested and demonstrated experimentally. Practically, to design a periodically layered structure for a specific application, a precise knowledge on the spectral response of the periodically layered structure is necessary. Various methods were developed to calculate the spectral response of the periodically layered structure. The transfer matrix approach [20] is one of the most popular methods, and it has been extended and modified [21-25] to calculate various types of the periodically layered structures. In this approach, the layered structure is divided into short segments with uniform grating parameters. The fundamental matrices are determined for each segment based on the coupled wave theory, and the spectral response characteristics of the layered structure is obtained by multiplying these fundamental matrices in certain phase conditions of the grating at the interface between two adjacent segments. The transfer matrix approach was also applied to calculate the light propagation in one-dimension photonic crystal with a negative permittivity and permeability, the photonic bandgap was found to be enhanced dramatically in these metamaterials [26]. Recently, Birge and Kärtner [27] demonstrated an inductive method to compute derivatives of reflection phase for layered media by using the transfer matrix formalism, which leads to an efficient way for accurately computing dispersion significantly faster than with standard finite-difference methods. The beam propagation method [28-31] is another flexible and broadly applicable numerical tool to characterize the beam propagation behaviors in periodically layered structures, where the distributed optical inhomogeneities of a periodically layered structure are approximated by a discrete sequence of physically and mathematically infinitesimally thin phase and/or polarization modulation layers, which is intervened with optically homogeneous layers of finite thickness. The stratified volume holographic optical elements [13-16] were suggested based on the concept of separating the volume holographic structure into a sequence of discrete thin modulation layers used in the beam propagation method. In a stratified volume holographic optical element, a sequence of thin photosensitive holographic recording layers are interleaved with photo-insensitive buffer layers. Although a grating recorded in any individual photosensitive layer exhibits Raman-Nath characteristics because of its thin thickness, a stratified volume holographic optical element with even a small number of photosensitive layers, each spaced from its neighbors by a buffer layer of appropriate thickness, shows a Bragg-like diffraction behavior. The finite-difference time-domain simulation code is a powerful numerical method to simulate the light propagation behaviors in various material systems. It was employed recently to calculate the propagation characteristics of a one-dimension photonic crystal with finite length and finite height [32].

In this paper, we have designed a periodically layered structure, a stratified and phase-shifted volume index grating (SPVIG), consisting of a sequence of discrete thick volume index gratings interleaved with optically homogeneous buffer layers. A recursion formula for the reflectance of the SPVIGs is derived, and its reflectance properties are studied under various conditions. As compared to a single uniform volume index grating (SG), an enhanced effect on the control of light group velocity with a high transmittance by using the SPVIGs is demonstrated.

and

$$\frac{\partial B_1(x)}{\partial x} = -i\kappa A_1(x)e^{i\Delta kx}, \quad (4)$$

respectively. Where $\kappa = \pi n_1/\lambda$ is the coupling constant, $\Delta k = 2k_0 - K$ is the momentum mismatch. The general analytical solutions for $A_1(x)$ and $B_1(x)$ can be written as

$$A_1(x) = (A_1(0) \cosh(sx) + C_1 \sinh(sx))e^{-i\Delta kx/2}, \quad (5)$$

and

$$B_1(x) = -\frac{i}{\kappa}e^{i\Delta kx} \frac{\partial A_1(x)}{\partial x}, \quad (6)$$

respectively. Where $A_1(0)$ is the amplitude of the incident light at $x = 0$, s is given by $s = (\kappa^2 - (\Delta k/2)^2)^{1/2}$, and C_1 is a parameter determined by the boundary conditions. Under the boundary condition $B_1(D) = 0$, the reflection coefficient of the grating layer is given by

$$r_1 = \frac{B_1(0)}{A_1(0)} = \frac{i\kappa \sinh(sD)}{s \cosh(sD) - i(\Delta k/2) \sinh(sD)}. \quad (7)$$

Now supposing we know the reflection coefficient r_N of a N -layer SPVIG with N grating layers interleaved with $N-1$ buffer layers, we will derive a recursion formula for the reflection coefficient r_{N+1} of a $(N+1)$ -layer SPVIG. Such a recursion technique for calculation of reflection coefficient is generally used in distributed feedback laser [33].

It is evident that the amplitude of the electric field $E_j(x)$ in the j -th grating layer is the summation of the forward and the backward propagation waves $E_j(x) = A_j(x)\exp(ik_0(x - (j-1)(D+d))) + B_j(x)\exp(-ik_0(x - (j-1)(D+d)))$. The amplitudes of the forward and backward propagation waves in the first layer are described by Eqs. (5) and (6), regardless of the layer number of the SPVIG. In each case, the parameter C_1 is determined by the boundary conditions at the two interfaces of the buffer layer sandwiched between the first and the second grating layers. These boundary conditions can be expressed as

$$A_1(D)e^{ik_0d} = A_2(D+d), \quad (8)$$

and

$$B_1(D) = B_2(D+d)e^{ik_0d}, \quad (9)$$

respectively. By combining the expression of the reflection coefficient of the N -layer SPVIG $r_N = B_2(D+d)/A_2(D+d)$, we obtain the parameter C_1 as a function of r_N

$$C_1 = \frac{i\kappa r_N \cosh(sD)e^{-i\Delta kD+2ik_0d} + i\frac{\Delta k}{2} \cosh(sD) - s \sinh(sD)}{-i\kappa r_N \sinh(sD)e^{-i\Delta kD+2ik_0d} - i\frac{\Delta k}{2} \sinh(sD) + s \cosh(sD)} A_1(0). \quad (10)$$

By substituting Eq. (10) into Eqs.(5) and (6), we obtain the recursion formula for the reflection coefficient r_{N+1} of the $(N+1)$ -layer SPVIG

$$r_{N+1} = \frac{B_1(0)}{A_1(0)} = \frac{sr_N \cosh(sD)e^{-i\Delta kD+2ik_0d} + i\frac{\Delta k}{2} r_N \sinh(sD)e^{-i\Delta kD+2ik_0d} + i\kappa \sinh(sD)}{-i\kappa r_N \sinh(sD)e^{-i\Delta kD+2ik_0d} - i\frac{\Delta k}{2} \sinh(sD) + s \cosh(sD)}. \quad (11)$$

Therefore the reflectance of the $(N+1)$ -layer SPVIG is $R_{N+1} = |r_{N+1}|^2$ and the transmittance T_{N+1} can be obtained through $T_{N+1} = 1 - R_{N+1}$. The recursion formula (11) provides a precise prediction of the characteristics of the reflectance spectra of the SPVIGs with a normal incident light. It is worthy of mention that for the case of oblique incidence the results will be different

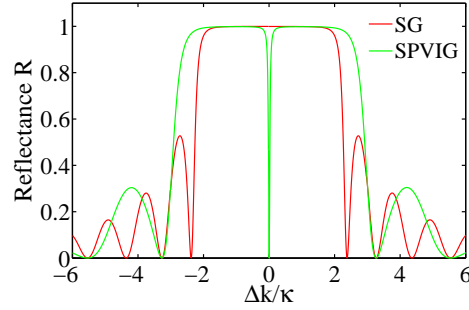


Fig. 2. Reflectance spectra of a SG (red) and a 2-layer SPVIG (green). The grating parameters for both cases are $\Lambda = 0.5 \mu\text{m}$ and $n_1 = 4 \times 10^{-4}$. Other parameters are set to be $D = 3 \text{ mm}$, $d = 2.25 \mu\text{m}$ and $n_0 = 1.55$, respectively. The thickness of the SG is 6 mm for comparison.

for the TE and the TM waves, however, a detailed discussion on the oblique incidence case deserves another full-length paper and is beyond the scope of this paper.

In the following section, we will discuss the characteristics of the reflectance spectra of the SPVIGs.

4. Characteristics of the reflectance spectra of SPVIGs

To study the characteristics of the reflectance spectra and to understand the effects of the buffer layers on the reflectance spectra, let us first consider the simplest SPVIG with $N=2$, where a buffer layer is sandwiched between two volume index grating layers. By substituting Eq. (7) into Eq. (11), we obtain the reflection coefficient for the 2-layer SPVIG

$$r_2 = \frac{i\kappa \sinh(sD) \left(1 + \frac{s \cosh(sD) + i \frac{\Delta k}{2} \sinh(sD)}{s \cosh(sD) - i \frac{\Delta k}{2} \sinh(sD)} e^{-i\Delta k D + i2k_0 d} \right)}{\frac{\kappa^2 \sinh^2(sD)}{s \cosh(sD) - i \frac{\Delta k}{2} \sinh(sD)} e^{-i\Delta k D + i2k_0 d} + s \cosh(sD) - i \frac{\Delta k}{2} \sinh(sD)}. \quad (12)$$

In the case with a Bragg-matched incident wavelength λ_0 for the volume index grating layer, i.e., $\Delta k = 0$, the reflection coefficient of the 2-layer SPVIG can be simplified to be

$$r_2 = \frac{i\kappa \sinh(sD) (1 + e^{i2k_0 d})}{\frac{\kappa^2 \sinh^2(sD)}{s \cosh(sD)} e^{i2k_0 d} + s \cosh(sD)}. \quad (13)$$

It is evident that the reflection coefficient r_2 is equal to zero under the condition $2k_0 d = (2m + 1)\pi$, where m is an integer. Therefore a transparency peak appears in the stop-band of the reflectance spectrum of the volume index grating, as shown in Fig. 2, where the reflectance spectrum of a 2-layer SPVIG is shown. Similar phenomena were also reported in phase-shifted fiber Bragg gratings [4, 5, 6, 7, 8]. In the simulation, the structure parameters for the 2-layer SPVIG are $n_0 = 1.55$, $n_1 = 4 \times 10^{-4}$, $\Lambda = 0.5 \mu\text{m}$, $\lambda_0 = 1.55 \mu\text{m}$, $D = 3 \text{ mm}$ and $d = 2.25 \mu\text{m}$, respectively. It is evident that such a transparency peak is a result of the interference between the forward waves and the backward waves reflected from the first and the second volume index grating layers. For comparison, the reflectance spectrum of a 6-mm SG with the same grating

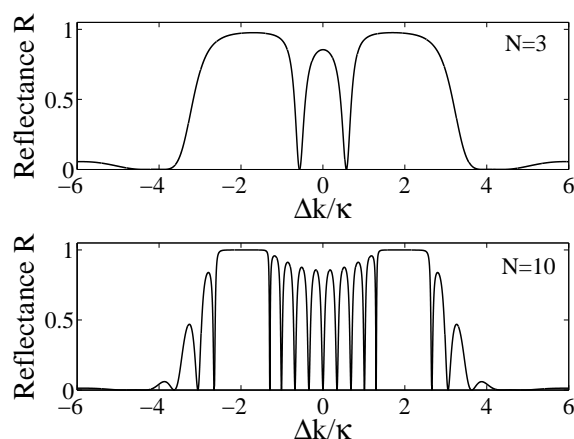


Fig. 3. The reflectance spectra of the SPVIGs with $N=3$ (a) and $N=10$ (b), respectively. The parameters for both cases are set to be $n_0 = 1.55$, $n_1 = 4 \times 10^{-4}$, $D = 2$ mm, $\Lambda = 0.5$ μm , and $d = 2.25$ μm , respectively.

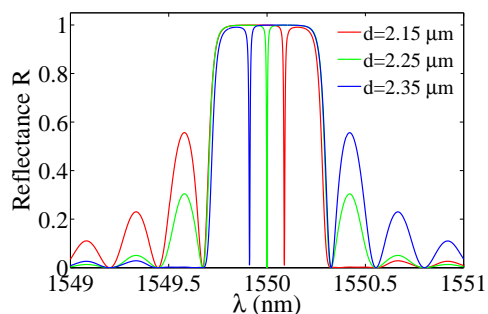


Fig. 4. Shift of the transparency wavelength within the stop-band by controlling the thickness of the buffer layer in a 2-layer SPVIG. The thicknesses of the buffer layers are 2.15, 2.25 and 2.35 μm for the red, green and blue curves, respectively. Other parameters are the same for three curves: $n_0 = 1.55$, $n_1 = 4 \times 10^{-4}$, $D = 3$ mm, and $\Lambda = 0.5$ μm , respectively.

parameters is also shown in Fig. 2. A broadening effect of the stop-band of the reflectance spectrum is also found for the SPVIG due to the interleave of the buffer layer.

The reflectance spectrum of a multilayer SPVIG can be calculated easily by using the recursion formula (see Eq. (11)). Figure 3 shows the reflectance spectra of a 3-layer (a) and a 10-layer (b) SPVIGs as examples. The structure parameters are the same as those of Fig. 2 except for $D = 2$ mm in Fig. 3. It is found that the number of the transparency peaks within the stop-band is equal to $N-1$, i.e., the number of the buffer layers in the structure. Therefore, two and nine transparency peaks appear in the reflectance spectra of the 3-layer and the 10-layer SPVIGs, respectively. On the other hand, a transparency peak appears at $\Delta k = 0$ when N is an even integer, whereas this is not the case when N is an odd integer. This is because the total phase-shift induced by the buffer layers of the SPVIGs is $(N-1) \times 2k_0d = (N-1) \times (2m+1)\pi$.

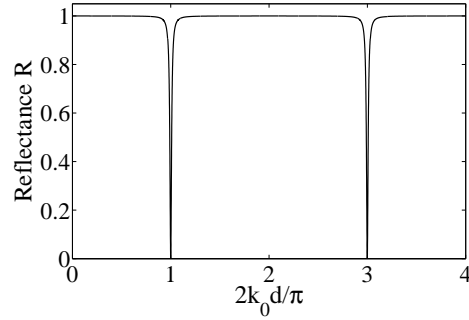


Fig. 5. The periodical transparency peaks at the Bragg-matched wavelength $\lambda_0 = 1.55 \mu\text{m}$ with the variation of the phase-shift $2k_0d$ induced by the buffer layer in a 2-layer SPVIG, where $n_0 = 1.55$, $D = 3 \text{ mm}$, $\Lambda = 0.5 \mu\text{m}$ and $n_1 = 4 \times 10^{-4}$, respectively.

An even integer N will result in a destructive interference, whereas an odd integer N leads to a constructive interference. It is evident that the coupled mode solution provides a clear physical insight into the formation of the band structure of the reflectance spectra.

The positions of the transparency peaks can be controlled by adjusting the phase-shift induced by the buffer layer. Figure 4 shows the possibility to shift the transparency wavelength by controlling the thickness of the buffer layer in a 2-layer SPVIG. The transparency wavelength is blue-shifted with an increase in the thickness of the buffer layer, while it is red-shifted with a decrease in the buffer layer thickness. On the other hand, at the Bragg-matched wavelength λ_0 the transparency peak appears periodically as a function of the phase-shift $2k_0d$ whenever the condition $2k_0d = (2m + 1)\pi$ is satisfied, as is shown in Fig. 5. These properties can be applicable to addressable wavelength filters, wavelength division multiplexing and de-multiplexing, and switching.

5. Dispersion properties of the SPVIGs and group velocity control

It is well known that a periodical structure is highly dispersive [1, 2] and such a dispersive property can be used to control the group velocity v_g of light beams [9, 34-38]. Lin et al. [35] studied the dispersive property of a SG and demonstrated the possibility to control the group velocity of light through a SG recorded in an iron-doped lithium niobate crystal. The group velocity of a SG can be expressed as [35]

$$v_g = v_p \frac{(\Delta k/2)^2 - \kappa^2 \cosh^2(sD)}{(\Delta k/2)^2 - \kappa^2 \frac{\sinh(sD)}{sD} \cosh(sD)}, \quad (14)$$

where $v_p = c/n_0$ is the phase velocity of lights in the host medium in the absence of the volume index grating. A group index $n_g = c/v_g$ of 7.5 was obtained in a 3.5-cm lithium niobate crystal with a refractive index modulation of 2.1×10^{-5} .

We study the dispersive properties of the SPVIG and find that the dispersion of the SPVIG is greatly enhanced as compared to that of the SG. Therefore, the SPVIG offers a great feasibility to control the group velocity of lights to a large extent through the design of the SPVIGs. In the following, we take a 2-layer SPVIG as an example without loss of the generality to illustrate the enhanced dispersion effect and its application to the control of the group velocity of light. Through a lengthy but straightforward calculation (see appendix A), we obtain the phase shift

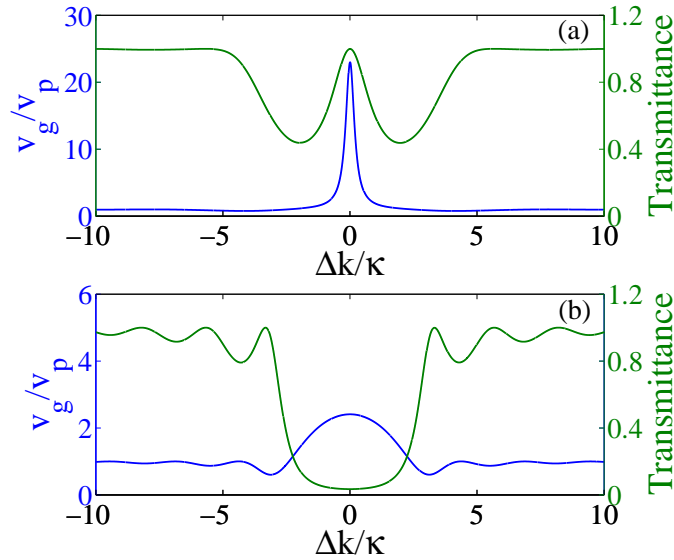


Fig. 6. The group velocity and the transmittance T of the light incident normally onto a 2-layer SPVIG (a) and a SG (b), respectively. The blue curves and the green curves are for the group velocity and the transmittance, respectively. The Bragg-matched wavelength is set to be $1.55 \mu\text{m}$. The parameters for the 2-layer SPVIG are set to be $n_0 = 1.55$, $D = 1.46 \text{ mm}$, $d = 0.25 \mu\text{m}$, $\Lambda = 0.5 \mu\text{m}$ and $n_1 = 4 \times 10^{-4}$, respectively. The grating parameters for the SG are the same as those of the SPVIG, and the thickness of the SG is equal to $2D+d$.

Φ of the transmitted light through a 2-layer SPVIG

$$\Phi = \frac{2\pi}{\Lambda}D + 2k_0d + \arctan\left(\frac{\sinh^2(sD)\sin\varphi + \sin\gamma\cos\gamma\sinh(2sD)}{\sinh^2(sD)\cos\varphi + \sin^2\gamma\cosh^2(sD) - \cos^2\gamma\sinh^2(sD)}\right). \quad (15)$$

Where we set $\sin\gamma = s/\kappa$, $\cos\gamma = \Delta k/2\kappa$, and $\varphi = \Delta kD - 2k_0d$ for convenience. The group velocity of lights through a 2-layer SPVIG can be obtained by differentiating the phase shift per unit length with respect to the angular frequency ω

$$v_g = (2D+d)\left(\frac{\partial\Phi}{\partial\omega}\right)^{-1}. \quad (16)$$

Figure 6 (a) shows the numerical results of the group velocity and the transmittance T of lights through a 2-layer SPVIG with $n_0 = 1.55$, $D = 1.46 \text{ mm}$, $d = 0.25 \mu\text{m}$, $\Lambda = 0.5 \mu\text{m}$ and $n_1 = 4 \times 10^{-4}$, respectively. For comparison, the group velocity and the transmittance of a SG with $n_0 = 1.55$, a thickness of $2D+d$, $\Lambda = 0.5 \mu\text{m}$ and $n_1 = 4 \times 10^{-4}$ are also shown in Fig. 6 (b). Note that we neglect the dispersion of the refractive index n_0 in the calculation because what we consider here is the dispersion induced by the structure of the refractive index distribution instead of the refractive index of the material itself. This is reasonable for most optical materials such as photorefractive lithium niobate crystals and optical fibers without involvement of the nonlinear effects. It is seen that superluminal light propagation is demonstrated at/near the Bragg-matched wavelength in both cases, while the group velocity in the 2-layer SPVIG case is faster by a factor of ~ 10 as compared to that in the SG case. Moreover, the transmittance of the superluminal lights in the 2-layer SPVIG case is larger than 80%, whereas that in the

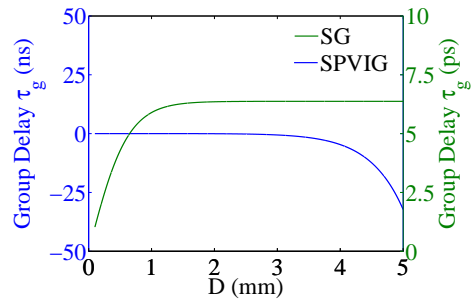


Fig. 7. The group delays τ_g of a 2-layer SPVIG (blue curve) and a SG (green curve) versus the variation of D . The wavelength is set at Bragg-matched and is at $1.55 \mu\text{m}$. The parameters for the 2-layer SPVIG are set to be $n_0 = 1.55$, $d = 0.25 \mu\text{m}$, $\Lambda = 0.5 \mu\text{m}$ and $n_1 = 4 \times 10^{-4}$, respectively. The thickness of the SG is equal to $2D+d$.

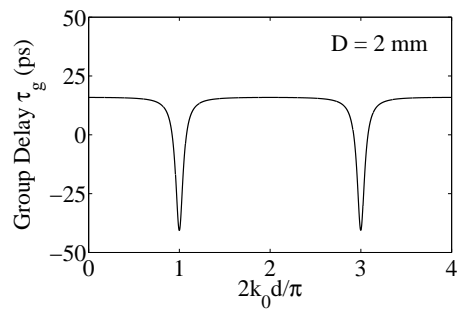


Fig. 8. The group delay τ_g of a 2-layer SPVIG versus the phase variation $2k_0d$ induced by the buffer layer. The wavelength is set to be Bragg-matched at $1.55 \mu\text{m}$. The parameters for the 2-layer SPVIG are set to be $n_0 = 1.55$, $D = 2 \text{ mm}$, $\Lambda = 0.5 \mu\text{m}$ and $n_1 = 4 \times 10^{-4}$, respectively.

SG case is less than 5% due to the Bragg-reflection effect. Figure 7 shows the group delay τ_g (defined as $\tau_g = L/v_g$, where L is the total thickness of the SPVIG or the SG) as a function of the thickness D for the 2-layer SPVIGs and the SGs at the Bragg-matched wavelength $\lambda_0 = 1.55 \mu\text{m}$. The parameters for n_0 , d , Λ and n_1 are set to be 1.55, $0.25 \mu\text{m}$, $0.5 \mu\text{m}$ and 4×10^{-4} , respectively. The thickness of the SG is $L = 2D + d$. It is seen that the group delay in the SG case increases first but then tends to be saturated with the increase of D . The group delay in the 2-layer SPVIG case varies first slowly but then becomes negative and decreases rapidly with the increase of D . A negative group delay of $\sim 30 \text{ ns}$ is possible with $D = 5 \text{ mm}$. This is because the transparency peak becomes sharper and sharper; therefore, the dispersion slope becomes steeper and steeper with increasing D in the 2-layer SPVIG case. Note that the time scale for the SPVIG is nano-second while that for the SG is pico-second in Fig. 7. Figure 8 illustrates the control of the group delay through the phase variation $2k_0d$ induced by the buffer layer. The parameters for the SPVIG is $n_0 = 1.55$, $D = 2 \text{ mm}$, $\Lambda = 0.5 \mu\text{m}$, and $n_1 = 4 \times 10^{-4}$, respectively. The operating wavelength is set to be Bragg-matched at $1.55 \mu\text{m}$. We see that, whenever the condition $2k_0d = (2m + 1)\pi$ is satisfied which corresponds to the appearance of the transparency peak at the Bragg-matched wavelength, a sharp increase in the group delay is observed. These results clearly illustrate the versatility and the effectiveness of the SPVIG on the control of the group velocity of light through the design of its structure parameters. Experiments on group velocity control through a 2-layer SPVIG by using a photorefractive lithium niobate crystal are currently going on in our laboratory. The photosensitive optical fiber could be an additional good material candidate to fabricate the stratified and phase-shifted volume index gratings.

6. Conclusion

In conclusion, we have obtained the recursion formula for the reflectance of the SPVIGs and studied the spectral characteristics of the SPVIGs based on the recursion formula. Transparency peaks appear within the stop-band of the volume index grating due to the interleave of the homogeneous buffer layers in the SPVIG. The spectral positions of the transparency peaks can be controlled through the phase-shift induced by the buffer layer. The dispersion slope is found to be very steep at/near the transparency peaks in the SPVIG and it can be used to control the group velocity of light to a large extent. The group delay experienced by the light through the SPVIG can be controlled by adjusting the phase shift induced by the buffer layer. Negative group delay in the order of tens of nano-seconds with high transmittance is possible with a centimeter-length SPVIG. Such properties can be applicable to addressable filter, wavelength division multiplexer and de-multiplexer, switching, and controllable optical delay/advance line. As compared to the SG, the SPVIG offers more feasibility and versatility to modify the spectral response and to control the group velocity.

Acknowledgments

This work is financially supported by the Key Project of Chinese Ministry of Education under grant 104054, the National Natural Science Foundation of China (grants 60308005, 60678021 and 10334010), the Program for New Century Excellent Talents in University under grant NCET-04-0234, the Program for Changjiang Scholars and Innovative Research Team in University, the Cultivation Fund of the Key Scientific and Technical Innovation Project, Ministry of Education of China under grant 704012, the Municipal International Cooperation Program of Tianjin under grant 06YFGHHZ00500, the National Basic Research Program of China under grant 2007CB307002, and CNKBRFSF under grant 2006CB921703.

Appendix

A. Derivation of the phase shift Φ of the transmitted light through a 2-layer SPVIG

The amplitude of the electric field $E_2(x)$ in the second grating layer is the summation of the forward and the backward propagation waves

$$E_2(x) = A_2(x)e^{ik_0(x-(D+d))} + B_2(x)e^{-ik_0(x-(D+d))}, \quad (17)$$

where $A_2(x)$ is

$$A_2(x) = (A_2(D+d) \cosh(s(x-(D+d))) + C_2 \sinh(s(x-(D+d)))) e^{-i\Delta k(x-(D+d))/2}, \quad (18)$$

and $B_2(x)$ satisfies

$$B_2(x) = -\frac{i}{\kappa} e^{i\Delta k(x-(D+d))} \frac{\partial A_2(x)}{\partial(x)}. \quad (19)$$

By combining the boundary conditions expressed by Eqs. (8) and (9), we obtain

$$C_2 = \frac{1}{s} \left(i\kappa B_1(D) e^{-ik_0 d} + i \frac{\Delta k}{2} A_1(D) e^{ik_0 d} \right). \quad (20)$$

Where $A_1(D)$ and $B_1(D)$ can be obtained by substituting Eqs. (7) and (10) into Eqs. (5) and (6) under the boundary condition $B_2(2D+d) = 0$. The amplitude $E_2(2D+d)$ is then expressed as

$$E_2(2D+d) = A_2(2D+d) e^{ik_0 D}, \quad (21)$$

where $A_2(2D+d)$ is

$$A_2(2D+d) = \frac{s^2}{\kappa^2} \frac{A_1(0)}{ARe - iAIm} e^{ik_0 d} e^{-i\Delta k D}, \quad (22)$$

with the parameters ARe and AIm being

$$ARe = \sinh^2(sD) \cos \varphi + \sin^2 \gamma \cosh^2(sD) - \cos^2 \gamma \sinh^2(sD) \quad (23)$$

and

$$AIm = \sinh^2(sD) \sin \varphi + \cos \gamma \sin \gamma \sinh(2sD), \quad (24)$$

respectively. By taking account of the propagation phase shift $k_0(D+d)$ induced by the first grating layer and the buffer layer, we obtain the phase shift Φ of the transmitted light through a 2-layer SPVIG shown by Eq. (15).